Journal of Physics:
Condensed Matter

**PAPER** • **OPEN ACCESS**

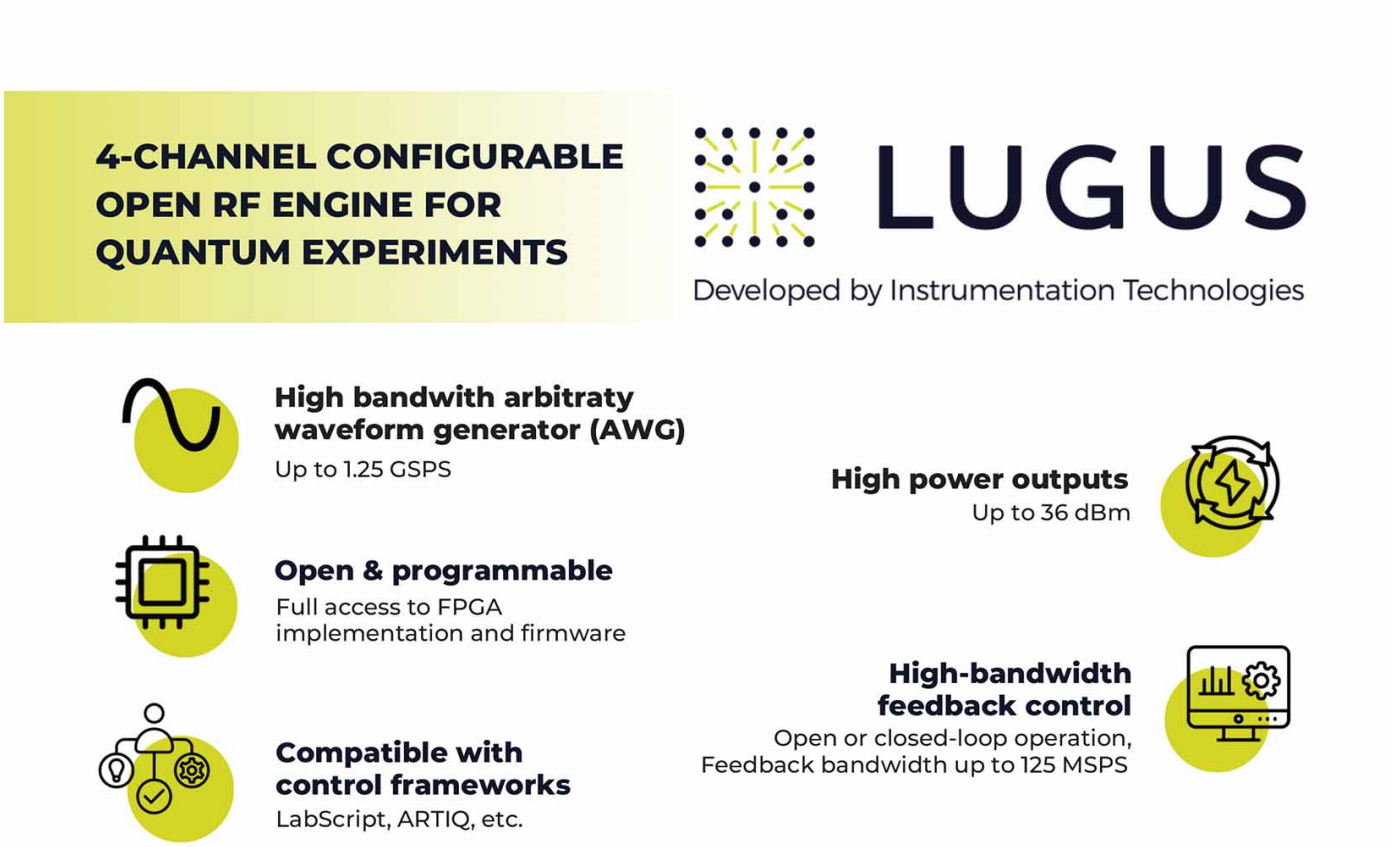
# The *E*1–*E*2 center in gallium arsenide is the divacancy

To cite this article: Peter A Schultz 2015 *J. Phys.: Condens. Matter* **27** 075801

View the article online for updates and enhancements.

You may also like

- Analysis of arsenic in raw and cooked rice by atomic absorption spectrophotometer
Silalahi Jansen, Rosa Tampubolon Sanggam Dera, MayriaSagala MargarethRuth et al.
- An Artificial Channel Purification Experiment for Arsenic-rich Drainage Water from the Abandoned Mine by using *Eleocharis acicularis*
Kenji Okazaki, Shusaku Yamazaki, Toshiyuki Kurahashi et al.
- Selective Separation of Arsenic from Arsenic-bearing Copper Dust by Vulcanization Reduction
Xuepeng Li, Juan Wang and Jun Chang




This content was downloaded from IP address 216.73.216.56 on 19/11/2026 at 09:12

OPEN ACCESS
IOP Publishing
Journal of Physics: Condensed Matter
J. Phys.: Condens. Matter **27** (2015) 075801 (6pp)
doi:10.1088/0953-8984/27/7/075801

# The *E*1–*E*2 center in gallium arsenide is the divacancy

**Peter A Schultz**

Multiscale Science, Sandia National Laboratories, Albuquerque, NM 87185-1322, USA

E-mail: paschul@sandia.gov

Received 22 August 2014, revised 26 September 2014
Accepted for publication 2 October 2014
Published 30 January 2015




**Abstract**

Based on defect energy levels computed from first-principles calculations, it is shown the $E1$–$E2$ center in irradiated GaAs cannot be due to an isolated arsenic vacancy. The only simple intrinsic defect with levels compatible with $E1$ and $E2$ is the divacancy. The arsenic monovacancy is reassigned to the $E3$ center in irradiated GaAs. These new assignments are shown to reconcile a number of seemingly contradictory experimental observations.

Keywords: gallium arsenide, defects, density functional theory

(Some figures may appear in colour only in the online journal)

## 1. Introduction

Performance of semiconductor electronic devices is dictated ultimately by the presence and behavior of point defects. A detailed knowledge of the properties and chemical evolution of those defects is crucial to the engineering of robust devices that operate effectively in normal operation conditions and under irradiation. In silicon, a vast, detailed understanding of defect behavior [1] has been developed, an result of extensive study over decades, and this has been of inestimable value in designing robust modern electronics. After silicon, gallium arsenide is perhaps the most studied semiconductor, with uses in a variety of devices. Despite early optimism [2] and notwithstanding intense effort over decades, definitive knowledge concerning even simple intrinsic defects in GaAs remains scanty. With electron paramagnetic resonance studies impaired in GaAs as a sensitive probe for the chemical structure of a defect [2, 3], theory proved invaluable in identifying the arsenic antisite $As_{Ga}$—an arsenic replacing a gallium atom in the lattice—as the defect responsible for the $EL2$ [4, 5], the dominant center in as-grown GaAs.

Electron irradiation is an effective approach to study primary defects in materials. The initial products of electron irradiation are simple intrinsic defects: vacancies and interstitials resulting from primary lattice displacements. The $EL2$, only observed in as-grown GaAs, has been identified as $As_{Ga}$. The identities of defect centers observed in irradiated GaAs have proven more inscrutable. In $n$-type GaAs, a series of levels, designated $E1$ through $E5$, have been observed in $e$-irradiated GaAs above mid-gap [2]. The $E1$ level that appears at 32–45 meV below the conduction band (CB) and the $E2$ level at 0.13–0.18 eV [3, 6–8] are demonstrated to be two distinct transitions of the same defect [3], and are usually attributed to $v_{As}$ [2]. The $E3$, $E4$, and $E5$ are transitions due to different defects, the $E3$ being the best characterized of these and is most commonly attributed to a $v_{As}$–$As_i$ pair.

Identification of defects beyond the $EL2$ has been hampered by the lack of an experimental tool to unambiguously determine and characterize the chemical structure of a defect associated with an energy level. Conversely, first-principles calculations, particularly well suited for determining defect structure, have been unable to predict defect levels with quantitative accuracy sufficient to identify defects. In this work, I apply a robust method for computing accurate defect energy levels [9] to simple intrinsic defects in GaAs and determine that long-standing assignments of defect energy levels in GaAs need to be reassessed. The radiation-induced $E1$–$E2$ center, formerly associated with the arsenic monovacancy $v_{As}$, cannot be $v_{As}$ and, instead, must be due to the divacancy $vv$. The $v_{As}$, no longer conscripted to account for the $E1$–$E2$ center, proves to give an apt account of the properties of the $E3$ center, once a site-shifting bistability is incorporated into a comprehensive description of $v_{As}$. These new assignments correlate with observed

Content from this work may be used under the terms of the Creative Commons Attribution 3.0 licence. Any further distribution of this work must maintain attribution to the author(s) and the title of the work, journal citation and DOI.

 © 2015 IOP Publishing Ltd Printed in the UK

behavior and reconcile seemingly contradictory experimental observations.

## 2. Methods

All density functional theory (DFT) calculations are performed using the Gaussian-basis pseudopotential code SeqQuest [10]. Exercising a new method for the accurate evaluation of energy levels of defects within a supercell approximation [9], we obtained all levels for all simple intrinsic defects of GaAs: both monovacancies and the divacancy, both antisites and the double antisite, and both single interstitials [11]. For silicon defects, this method predicted defect energy levels with an average accuracy of 0.1 eV and maximum error of ∼0.2 eV. In GaAs, the computed span of defect levels, $\gtrsim$1.5 eV [12], almost exactly matches the experimental band gap of 1.52 eV [13]. Furthermore, $As_{Ga}$ calculations quantitatively match $EL2$ properties, e.g. the computed (0/1+) level is mid gap, 0.73 eV above the valence band, the (1 + /2+) 0.24 eV below that [11]. This accuracy is comparable to the silicon defect study and validates using this computational model for accurate defect simulations in GaAs.

The analysis here (except where noted) focuses on the results of local density approximation (LDA) [14] simulations using Ga pseudopotentials with 3$d$ electrons in the core, in 216-site cubic supercells with a $2^3$ $k$-sampling grid offset from the Γ-point. Computed energy levels for all intrinsic defects were also extrapolated from 512-site, and also selected 1000-site (both these with $2^3$ $k$-sampling) supercell calculations, to demonstrate that the computed levels were converged to the asymptotic dilute limit. The results extrapolated from 512-site cells matched to within ∼0.05 eV of the same levels extrapolated from 216-site supercells, demonstrating robust control of finite size effects, $k$-point sampling, and boundary conditions. For the defects discussed here, the conclusions are insensitive to use of a generalized gradient approximation such as PBE [15] rather than the LDA, or including the Ga 3$d$ electrons as valence electrons.

## 3. Results and analysis

The presence of the divacancy in GaAs has historically been dismissed, due to early calculations predicting a high $vv$ formation energy that precluded any significant population in equilibrium conditions [16], and positron annihilation calculations that yielded predictions of lifetimes in $vv$ incompatible with any experimental observation in irradiated GaAs [17]. In the current calculations, $vv$ takes charge states from (2+) to (4−). The formation energy of $vv(0)$, 4.19 eV, only slightly exceeds $v_{As}(0)$, 3.55 eV [11]. The previously unanticipated (4−) and (3−) charge states of the divacancy prove pivotal in explaining the radiation-induced $E1$–$E2$ centers. The $v_{As}$ takes charge states from (3+) to (3−). A unified treatment of a site-shift bistability in the description of the arsenic vacancy proves crucial in accounting for its observed behavior. Structural changes for the negative charge states and all computed levels for these defects is illustrated in figure 1.

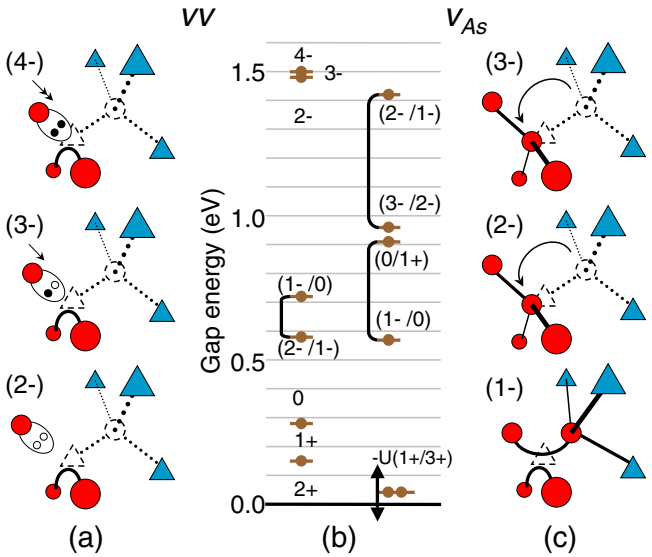



**Figure 1.** Schematic illustration of crucial features of the $vv$ and $v_{As}$ model for the $E1$–$E3$ centers in irradiated GaAs. ($a$) Bonding in the highly negative $vv$ charge states that result in the levels near the CB. The (blue) triangles depict arsenic atoms and (red) circles depict gallium atoms. The open shapes depict vacated sites. ($b$) Defect level diagram for $vv$ and $v_{As}$. The solid lines connect the levels of $-U$ systems. ($c$) Bonding in the $v_{As}$ charge states responsible for levels near the CB. The global site-shift bistability occurs between $v_{As}(1-)$ and $v_{As}(2-)$, as a Ga adjacent to the simple As vacancy hops into the vacant site.

The $vv$ can be described usefully as a $v_{Ga}$–$v_{As}$ pair. The $vv(2-)$ has three full As lone pairs on the $v_{Ga}$ side. The two electrons on the $v_{As}$ side form a stretched Ga–Ga bond pair, illustrated in figure 1($a$). The remaining trivalent Ga retreats from the vacant site. Adding an electron occupies the dangling bond on this Ga, causing it to pucker inwards by 0.6 Å in the $vv(3-)$. The $vv$ accommodates yet another electron in the $vv(4-)$, puckering this Ga another 0.2 Å inwards. The resulting $vv(4 - /3-)$ and $vv(3 - /2-)$ levels are closer to the CB than any level from any other simple intrinsic defect. The next lower $vv$ level is too distant from the conduction band (CB) to be of interest here; the $vv(2 - /0)$ is a negative-$U$ transition near mid-gap, the inversion of charge transition levels (the $-U$) triggered by the dissociation of the Ga–Ga bond pair across the $v_{As}$ side of the divacancy.

The arsenic vacancy proves globally bistable, as illustrated in figure 1($c$), between a simple $v'_{As}$ and a nearest-neighbor $v_{Ga}$–$Ga_{As}$ pair obtained by an adjacent Ga atom shifting from its lattice site to the vacant site, a structure designated $v^*_{As}$. The four valence electrons of $v'_{As}(1-)$ couple into two Ga–Ga bond pairs in the ground state of $v_{As}(1-)$, with $D_{2d}$ symmetry. The ground state of $v_{As}(2-)$ and $v_{As}(3-)$ is the site-shifted $v^*_{As}$. The large lattice relaxation (the site shift) reverses the standard order of the transitions, forming a $-U$ system: $v_{As}(3 - /2-)$ is more strongly bound than $v_{As}(2 - /1-)$.

The calculated $v_{As}$ and $vv$ levels are presented in figure 1($b$). The $v_{As}$ does not have two distinct levels in the upper part of the gap, only a single $-U$ transition. This $-U(3 - /1-)$ transition is much deeper in the gap than the $E1$ and $E2$ levels. The $E1$ and $E2$ were originally both

identified as acceptor levels [6], but negative charge states proved incompatible with the (1−), (0), and (1+) charge states required for a $v_{As}$ model to be consistent with the results of positron experiments [18]. My computed $v_{As}(1-/1+)$ charge transition is a single $-U$ energy level near mid-gap. It is farther from the CB (and $E1$ and $E2$) than the maximum error seen in any LDA (or PBE) defect level calculation. The $v_{As}$ cannot be responsible for $E1$ and $E2$.

The $vv(4-/3-)$ and $vv(3-/2-)$ transitions are the only viable candidates for $E1$ and $E2$. These transitions are near the CB, above all the computed $v_{As}$ levels. No other simple intrinsic defect has computed levels within 0.5 eV of the CB edge. These $vv$ levels are ideally located to correspond to $E1$ and $E2$, especially once spin polarization is included. Spin lowers the $vv(3-)$ energy by 0.03 eV, increasing the splitting between $vv(4-/3-)$ and $vv(3-/2-)$ from 0.02 eV to 0.08 eV, good agreement with the observed 0.10 eV splitting between $E1$ and $E2$ observed in experiment, either $E_c - .032$ and $E_c - .129$ eV [8] or $E_c - .045$ and $E_c - .140$ eV [3]. To confirm the assignment of $E1$ and $E2$ to $vv$, a few other experimental observations must be explained.

One early experiment proposed the divacancy was responsible for the positron lifetimes associated with the $E1$ and $E2$ [19]. However, this assignment was rejected in later studies, replaced with a $v_{As}$ model, partially based on analyses of positron studies. The positron annihilation lifetime calculated for $vv$ by Puska and Corbel [17] was much longer than that observed for $E1$ and $E2$. This result was used to reject the $vv$ model [2, 7]. However, those lifetime calculations used a $vv$ structure where the atoms relaxed *outwards*, and did not consider (4−) and (3−) charge states. The atoms in $vv(4-)$ and $vv(3-)$ relax strongly *inwards*, and a smaller vacancy volume generally leads to a shorter positron lifetime.

The observed position trapping coefficient decreases after emitting one electron ($E1$), and disappears after emitting a second electron ($E2$) [18]. This observation motivated the reanalysis of the charge states in the $v_{As}$ model: the neutral $v_{As}(0)$ would bind a positron less well than the negative $v_{As}(1-)$, positive charge in $v_{As}(1+)$ would repel a positron, rendering the center invisible to positron annihilation spectroscopy. This progression of positron trapping behavior with charge state can be explained just as well in a $vv$ assignment to this defect center, with transitions from $vv(4-)$ to $vv(3-)$ to $vv(2-)$.

In the (4−), (3−), and (2−) charge states, the three As lone pairs on the $v_{Ga}$ side of the $vv$ are populated by six electrons. The electron charge changes occur on the $v_{As}$ side, evidenced by the sequential structural rearrangements that occur there. In bulk GaAs, each As contributes $\frac{5}{4}$ electrons to each bond, Ga $\frac{3}{4}$ electrons. In a nominally neutral divacancy, therefore, each Ga dangling bond has $\frac{3}{4}$ electrons. In $vv(4-)$, the $v_{As}$ side distributes four valence electrons among three Ga dangling bonds in a Ga–Ga bond pair and two electrons in a pyramidal Ga lone pair, resulting in a nominal charge of $-\frac{7}{4}$. Going from $vv(4-)$ to $vv(3-)$ removes an electron from the Ga lone pair, causing that Ga atom to retreat slightly from the vacancy, reducing the charge on the $v_{As}$ side to $-\frac{3}{4}$. The next electron, to form the $vv(2-)$, also comes out of this Ga lone pair, the now-trivalent Ga retreats strongly from the vacancy, toward a planar $sp^2$-configuration, making the $v_{As}$ side a slightly positive $+\frac{1}{4}$. This net positive charge makes it repulsive for positron capture. Furthermore, the $v_{Ga}$ side of $vv$ is highly negative, nominally $-\frac{9}{4}$, making the $v_{Ga}$ side much more attractive for a positron than the now-positive $v_{As}$ side. Positrons trapped on the $v_{Ga}$ side of $vv$ are invisible to spectroscopy: the isolated $v_{Ga}(3-)$ has never been observed, suggesting that positron trapping at full As lone pairs leads to short positron lifetimes indistinguishable from annihilation in bulk GaAs. Hence, in positron annihilation experiments, $vv$ mimics a bare $v_{As}$, with an offset in the total charge state. The $vv$ model for $E1$ and $E2$ reconciles the original experiments that identify these as acceptors [6, 7] and positron experiments suggesting the lowest state was positively charged [18]. Positron lifetime calculations should be repeated with these new $vv$ charge states and the correct inward-relaxed structures.

No longer conscripted to explain $E1$ and $E2$, the $v_{As}$ is now free to be assigned elsewhere. I propose that the $E3$ center in irradiated GaAs [3], asserted to be the same as (or very similar to) the $EL6$ center seen in semi-insulating as-grown GaAs, [20], is the $v_{As}$. The $E3$ center is known to be a primary defect of displacement damage—it must be an intrinsic defect—and is an important recombination center in GaAs [21]. The $E3/EL6$ energy level is reported to be 0.27–0.38 eV below the conduction band edge [3, 20–25]. The only viable candidate in the computed survey of intrinsic defect levels is the $-U$ $v_{As}(3-/1-)$ transition, at roughly −0.3 eV in LDA (−0.35 eV in PBE), where this defect will emit two electrons midway between the $(3-/2-)$ and $(2-/1-)$ energy levels. With the divacancy assigned to the $E1$ and $E2$, no other intrinsic defects have candidate levels this high in the band gap; all other computed intrinsic defect levels are more than 0.2 eV lower, and hence farther than the observed maximum error of 0.2 eV. The LDA (and PBE) calculations with these new assignments agree with the experimental observations for $E1$–$E2$ and $E3$ to within 0.1 eV.

An early LDA study using 216-site supercells [26] reports $v_{As}$ charge states up to (3−), predicting that the $(2-/1-)$ and $(3-/2-)$ defect levels are almost equal, nearly $-U$, high in the gap, which could be possibly consistent with an interpretation of the $v_{As}$ highest two levels being associated with the $E1$–$E2$ levels. A more recent hybrid screened exchange (HSE) study using 64-site defect cells [27] reports their computed defect levels for the $v_{As}(3-/2-)$ and $(2-/1-)$ transitions near the conduction band, and assert these correspond with the observed $E1$–$E2$ transitions, apparently confirming the classic association of the $E1$–$E2$ levels with the arsenic vacancy. The current results can reconcile these computational observations as well. The essence of the analysis is illustrated in the computed level diagrams of figure 2, In these, the computed level diagrams of $v_{As}$ near the CB are depicted, for (*a*) $v_{As}$ restricted to a paired-$D_{2d}$ distortion (as in the HSE study [27]), then (*b*) switching to the ground state $v'_{As}$ structures into the resonant-$D_{2d}(3-)$ ground state, and then (*c*) the full $v_{As}$ energy level diagram that includes the $v^*_{As}$ site shift.

Earlier studies [11, 26] suggest that 216-site cells are necessary to get reliable results for defects, particularly

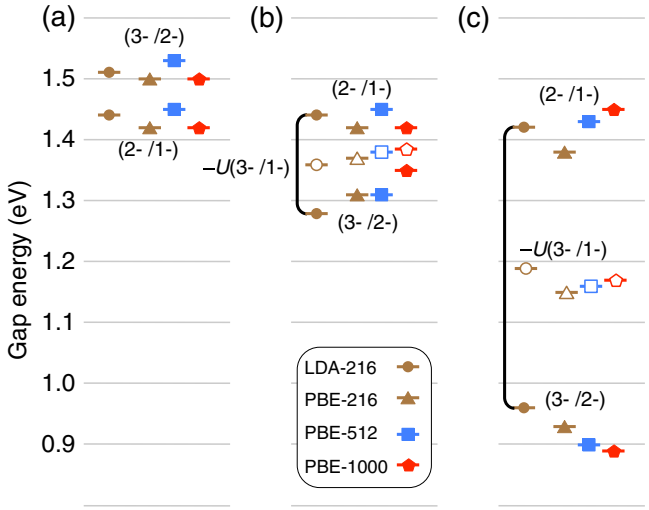



**Figure 2.** Computed level diagrams for the $v_{As}$ in the upper half of the GaAs band gap: (*a*) restricted to paired-$D_{2d}$ in simple vacancy $v'_{As}$; (*b*) traversing the lower energy resonant-$D_{2d}$ in $v'_{As}(3-)$; (*c*) the full thermodynamic energy levels for $v_{As}$, that traverses the site-shifted $v^*_{As}$ ground state in the (2−) and (3−). The computed LDA energy levels extrapolated from 216-site supercells are given in (brown) circles. The PBE results in 216-site cells are marked with (brown) triangles, 512-site cells with (blue) squares, and 1000-site cells with (red) pentagons. Restricted to the paired-$D_{2d}$ structure, the $v'_{As}$ gives two levels nears the CB edge. Traversing the ground state structures instead causes inverted $-U$ transitions, which would exhibit a single thermodynamic energy level in experiments, a double-electron emission midway between the computed charge transitions (open symbols).

for subtle relaxations around vacancies. The recent HSE results [27] reproduce very well our results with semilocal functionals, if one restricts the $v_{As}$ vacancy to just the paired-$D_{2d}$ structure. With either LDA or PBE, the $v'_{As}(3-/2-)$ level for the paired-$D_{2d}$ is right at the CB edge, with the $(2-/1-)$ slightly below, as seen in figure 2(*a*). However, earlier LDA results [11, 26], using larger 216-site cells with converged $2\times2\times2$ *k*-point sampling indicate that the resonant-$D_{2d}$ structure is favored over the paired-$D_{2d}$ for $v_{As}(3-)$, here, by 0.24(0.29) eV for LDA(PBE). The immediate consequence is that the $v_{As}(3-/1-)$ transition becomes $-U$, as depicted in figure 2(*b*), even before considering a site shift, already making it an unlikely match for the $E1$ and $E2$ levels. The results for a sequence of supercells of increasing size in figure 2 indicates that this result is converged to the bulk asymptotic limit with 216-site supercells.

Moreover, these calculations indicate that the site-shifted $v^*_{As}(3-)$ and $v^*_{As}(2-)$ are both favored over the simple arsenic vacancy $v'_{As}$. For the (3−), the $v^*$ is favored over the resonant-$D_{2d}$ by 0.34(0.42) eV for LDA(PBE); for the (2−), by 20–40 meV over the paired-$D_{2d}$ (the resonant-$D_{2d}(2-)$ is higher yet by ∼0.15 eV). This magnifies the $-U$ effect for the $(3-/1-)$ transition, and lowers the associated double-emission thermodynamic energy level to 0.30–0.35 eV below the CB edge, as depicted in figure 2(*c*). It is impossible that this thermodynamic level can correspond to the $E1$ and $E2$ near the CB edge, and it is in extraordinarily good agreement with the observed $E3$ level. That both the LDA and PBE give nearly identical results lends further confidence to this prediction.

This unified defect level model creating this $-U$, incorporating this site-shift, is dependent upon this site-shift being thermally accessible within an energy level measurement; otherwise they would be observed as two separate defects. My computations indicate the site-shifting barriers are very small. As the site-shifted $v^*_{As}(3-)$ loses electrons, it becomes less favored with respect to $v'_{As}$. The $v^*_{As}(1-)$ starting with the $v^*_{As}(2-)$ atomic configuration collapses to the ground state $v'_{As}(1-)$ without a barrier, in both LDA and PBE, in all supercells, from 216-site through 1000-site. Conversely, postulating that a electron filling pulse starting with the $v'_{As}(1-)$ could conceivably become trapped in the simple vacancy in the (2−) or even the (3−) charge state (not finding a path to the more stable $v^*$), the barrier from the $v'$ to $v^*$ for these charge states is also relevant. Saddle point barrier calculations reveal that the simple $v'$ has only a very small radius of stability against shifting into a $v^*$—a very small distortion of a neighbor toward the vacant site places the configuration on a downhill path to the lower energy site-shift—regardless of whether it is in the (2−) or (3−) charge state, with both LDA and PBE. The computed barrier for a site shift from $v'_{As}(2-)$ to $v^*_{As}(2-)$ is ∼0.1 eV, the barrier from $v'_{As}(3-)$ to $v^*_{As}(3-)$ is less than 0.07 eV. The $v'_{As}$ and $v^*_{As}$ must both be included in a unified treatment of $v_{As}$ defect levels.

Further experimental information also supports the notion of a larger $-U$ transition. The $EL6$ emission exhibits a large Franck–Condon factor, 0.6 eV, indicating this transition is associated with a large lattice relaxation [22]. It was later shown that the $EL6$ was but one of several emission peaks from a single defect: the intensities could be shifted between the $EL5$–$EL6$–$EL7$ family of levels by varying the filling pulse length in DLTS (deep-level transient spectroscopy), indicating a single $DX$-like center was responsible for these levels [25]. The predicted $-U$ $v_{As}(3-/1-)$ has a $DX$-like lattice relaxation, this transition involves a Ga atom hopping between two sites, from $v'_{As}$ into $v^*_{As}$, as illustrated in figure 1(*c*). Therefore, $v_{As}$ is compatible with known observations of the $E3$ and $EL6$ centers.

Identification of $E3$ with $v_{As}$ vindicates treating the $Ga_{As}$–$v_{Ga}$ pair as a bistable form of the simple As vacancy, including it in computing levels for $v_{As}$. The calculations demonstrated that $v_{Ga}$ also exhibits a site-shift bistability [11], as originally proposed by Baraff and Schlüter [28]. These unified descriptions might be crucial to understand fermi-level pinning in GaAs: the site-shifting, charge-switching vacancies are the basis of an amphoteric native defect model for understanding many phenomena in GaAs [29, 30]. Though aspects of this amphoteric model are contested [31], our calculations confirm both monovacancies do exhibit the necessary features.

As shown in figure 1(*b*), both $vv$ and $v_{As}$ are computed to have donor levels near the valence band edge. Levels measured in *p*-type GaAs could be consistent with these. It has been hypothesized that the $H0$–$H3$ traps observed in irradiated GaAs were other transitions of the same defects responsible for $E1$–$E3$ [2, 3], and the results here suggest this hypothesis is likely correct. However, absent other discriminating evidence, definitive assignment of those observed hole traps to $vv$ and $v_{As}$ on the basis of defect level matching alone would be more

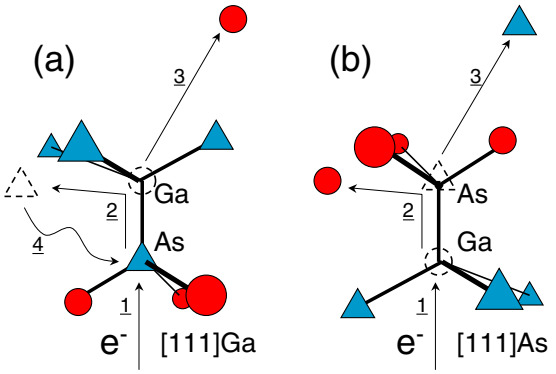



**Figure 3.** Schematic illustration of shadowing anisotropy leading to $vv$ selectivity for a [1 1 1]As direction ($b$) as opposed to ($a$) [1 1 1]Ga-direction incident electron beam, when incorporating differential diffusivities of interstitials. For low energy displacements, the incident electron, **1**, causes the front atom to recoil, **2**, imparting most of its momentum to the knocked-on shadowed atom, **3**, ejecting it farther from the vacancy. If the front atom is Ga ($b$), the nearby $Ga_i$ is trapped, leaving behind $vv$, appearing to be a 'As sublattice' defect. If the front atom is As ($a$), the nearby $As_i$ is more likely to be recaptured, **4**, by the $vv$, forming $v_{Ga}$.

speculative, as other intrinsic defects are computed to also have candidate levels in the lower half of the band gap [11] and could, in principle, be responsible for those hole traps.

In electron radiation experiments, the $E1$–$E3$ and $E3$ traps were determined to be from defects with atoms displaced from the arsenic sublattice [2], based upon (1) an analysis of the expected anisotropy of defect production rates, a shadowing effect, from [1 1 1]-directed electron beams [32], and (2) these traps being annealed by pair-recombination in first-order kinetics, presumably through annihilation by mobile $As_i$. Identification on the As sublattice was a central motivation for originally assigning $v_{As}$ to $E1$ and $E2$ [2], and appears inconsistent with a $vv$ model for this center. Incorporating a differential diffusivity for ejected Ga and As interstitials into this simple billiard-ball analysis results in an anisotropy selective for $vv$ on what appears to be the As sublattice.

The $Ga_i$ diffuses with thermal barriers of ∼1 eV [11, 33, 34]. Experiment inferred a 0.5 eV migration energy for $As_i$, confirmed in these DFT calculations [11]. In addition, the calculations indicate $As_i$ will diffuse athermally, sequential capture of electron and holes driving the arsenic interstitial through the lattice [11]. Under $e$-irradiation, with copious carriers, athermal migration will be activated. A $Ga_i$ ejected in a radiation-induced displacement is more likely to remain displaced. An $As_i$ displaced nearby has a greater probability of being recaptured by the (di)vacancy. Hence, a shadowing anisotropy results through the more or less distant ejection of $As_i$, as illustrated in figure 3. In one direction, the more distant $As_i$ often escapes, resulting in more $vv$ (and some $v_{As}$). In the reverse direction, the nearer $As_i$ is often recaptured, resulting in more $v_{Ga}$ (and only some $vv$). The key corollary is to note that, to this date, $v_{Ga}$ *has been invisible to electronic probes*, so that it would not be detected if it were present, hence capture of a $As_i$ by $vv$ would cause it to vanish. The $v_{Ga}$ has no levels above mid-gap, does not appear among the electron traps in $n$-type GaAs.

The threshold energy for displacement leading to generation of $E1$–$E2$ has been determined to be ∼10 eV [35]. By analogy to irradiated silicon, this was taken to be a single displacement, and lack of a second threshold at twice this energy suggesting the double-displacement, the divacancy, was absent. The results here, compelling evidence supporting the identification of the $vv$ with $E1$–$E2$, suggest that the assumptions that went into generalizing this threshold analysis from elemental silicon to a binary GaAs need to be reexamined, that the simple analogy to irradiated silicon is not quantitative.

## 4. Conclusions

In conclusion, the $E1$–$E2$ center in GaAs is determined to be due to the divacancy, on the basis of quantitative calculations of defect energy levels, and a detailed analysis of other experimental data. The standard model, $v_{As}$, cannot be responsible for $E1$ and $E2$ in GaAs. The $v_{As}$, instead, gives an apt description of the $E3$ ($EL6$) center. Previously unanticipated negative charge states for $vv$ and a unified description of a site-shift bistable $v_{As}$ are key insights needed to identify these traps. These assignments reconcile what had been seemingly conflicting experimental observations. Density functional theory supercell methods, using conventional semi-local functionals, are now accurate enough to make firm identifications of defects through defect level positions, adding $v_{As}$ and $vv$ to $As_{Ga}$ ($EL2$) as intrinsic defects that are unambiguously identified in GaAs.

## Acknowledgments

I thank Anatole von Lilienfeld for assistance in the calculations. I am very grateful to R Fleming and D Lang for innumerable enlightening insights regarding the interpretation of the vast experimental literature in irradiated GaAs. Sandia is a multiprogram laboratory operated by Sandia Corporation, a Lockheed Martin Company, for the United States Department of Energy's National Nuclear Security Administration under contract DE-AC04-94AL85000.

## References

[1] Pilcher P 2004 *Intrinsic Point Defects, Impurities, and Their Diffusion in Silicon* (New York: Springer)
[2] Bourgoin J C, Bardeleben H J and Stiévenard D 1988 Native defects in gallium arsenide *J. Appl. Phys.* **64** R65
[3] Pons D and Bourgoin J C 1985 Irradiation-induced defects in GaAs *J. Phys. C: Solid State Phys.* **18** 3839
[4] Dabrowski J and Scheffler M 1988 Theoretical evidence for an optically inducible structural transition of the isolated As antisite in GaAs: identification and explanation for of $EL2$? *Phys. Rev. Lett.* **60** 2183
[5] Chadi D J and Chang K J 1988 Metastabiliy of the isolated arsenic-antisite defect in GaAs *Phys. Rev. Lett.* **60** 2187
[6] Loualiche S, Nouailhat A, Guillot G and Lannoo M 1984 Interpretation of deep-level optical spectroscopy and deep-level transient spectroscopy data: application to irradiation defects in GaAs *Phys. Rev.* B **30** 5822
[7] Corbel C, Stucky M, Hautojärvi P, Saarinen K and Moser P 1988 Positron-annihilation spectroscopy of native vacancies in as-grown GaAs *Phys. Rev.* B **38** 8192

[8] Lai S T and Nener B D 1994 Annealing behavior of deep-level defects in 1 MeV electron-irradiated GaAs *J. Appl. Phys.* **75** 2354

[9] Schultz P A 2006 *Phys. Rev. Lett.* **96** 246401

[10] Schultz P A SeqQuest code (unpublished) see http:/dft.sandia.gov/Quest

[11] Schultz P A and von Lilienfeld O A 2009 Simple intrinsic defects in gallium arsenide *Modelling Simul. Mater. Sci. Eng.* **17** 084007

[12] Schultz P A and Edwards A H 2014 Modeling charged defects inside density functional theory band gaps *Nucl. Instrum. Methods* B **327** 2

[13] Vurgaftman I, Meyer J R and Ram-Mohan L R 2001 Review of band gap parameters for compound semiconductors *J. Appl. Phys.* **89** 8515

[14] Perdew J P and Zunger A 1981 Self-interaction correction for density-functional approximations for many-electron systems *Phys. Rev.* B **23** 5048

[15] Perdew J P, Burke K and Ernzerhof M 1996 Generalized gradient approximation made simple *Phys. Rev. Lett.* **77** 3865

[16] Northrup J E and Zhang S B 1994 Energetics of the As vacancy in GaAs: the stability of the 3+ charge state *Phys. Rev.* B **50** 4962

[17] Puska M J and Corbel C 1988 Positron states in Si and GaAs *Phys. Rev.* B **38** 9874

[18] Saarinen K, Hautojärvi P, Lanki P and Corbel C 1991 Ionization levels of As vacancies in as-grown GaAs studied by positron-lifetime spectroscopy *Phys. Rev.* B **44** 10585

[19] Dannefaer S and Kerr D 1986 Vacancy interactions in GaAs *J. Appl. Phys.* **60** 591

[20] Hashizume T and Nagabuchi H 1989 Characterization of deep electron states in LEC grown GaAs materials *Semicond. Sci. Technol.* **4** 427

[21] Fang Z Q, Schlesinger T E and Milnes A G 1987 Evidence for EL6 ($E_c - 0.35$ eV) acting as the dominant recombination center in *n*-type horizontal Bridgman GaAs *J. Appl. Phys.* **61** 5047

[22] Chantre A, Vincent G and Bois D 1981 Deep-level optical spectroscopy in GaAs *Phys. Rev.* B **23** 5335

[23] Martin G M, Estéve E, Langlade P and Makram-Ebeid S 1984 Kinetics of formation of the midgap donor $EL2$ in neutron irradiated GaAs materials *J. Appl. Phys.* **56** 2655

[24] Min S K, Kim E K and Cho H Y 1988 Abnormal behavior of midgap electron traps in HB-GaAs during thermal annealing *J. Appl. Phys.* **63** 4422

[25] Reddy C V, Luo Y L, Fung S and Beling C D 1998 $DX$-like properties of the $EL6$ defect family in GaAs *Phys. Rev.* B **58** 1358

[26] El-Mellouhi F and Mousseau N 2005 Self-vacancies in gallium arsenide: an *ab initio* calculation *Phys. Rev.* B **71** 125207

[27] Komsa H-K and Pasquarello A 2012 Intrinsic defects in GaAs and InGaAs through hybrid functional calculations *Physica* B **407** 2833

[28] Baraff G A and Schlüter M 1985 Bistability and metastability of the gallium vacancy in GaAs: actuator of $EL2$? *Phys. Rev. Lett.* **55** 2340

[29] Walukowski W 1989 Amphoteric native defects in semiconductors *Appl. Phys. Lett.* **54** 2094

[30] Ky N H and Reinhart F K 1998 Amphoteric native defect reactions in Si-doped GaAs *J. Appl. Phys.* **83** 718

[31] Chen C-H and Tan T Y 1995 On the validity of the amphoteric-defect model in gallium arsenide and a criterion of Fermi-level pinning by defects *Appl. Phys.* A **61** 397

[32] Pons D 1984 Anisotropy of defect introduction by electron irradiation of compound semiconductors *J. Appl. Phys.* **55** 2839

[33] Malouin M-A, El-Mellouhi F and Mousseau N 2007 Gallium self-interstitial relaxation in GaAs: an *ab initio* characterization *Phys. Rev.* B **76** 045211

[34] Levasseur-Smith K and Mousseau N 2008 Numerical characterization of the Ga interstitial self-diffusion mechanisms in GaAs *J. Appl. Phys.* **103** 113502

[35] Pons D, Mooney P M and Bourgoin J C 1980 Energy dependence of deep level introduction in electron irradiated GaAs *J. Appl. Phys.* **51** 2038